Pergamon

Int. J. Solids Structures Vol. 35, Nos 31–32, pp. 4191–4203, 1998

0020-7683/98 $19.00 + .00

PII: S0020-7683(97)00309-0

CHARACTERISTIC STRENGTH OF QUASI-BRITTLE MATERIALS

J. F. LABUZ*
Department of Civil Engineering, University of Minnesota, Minneapolis MN 55455, U.S.A.

and

L. BIOLZI
Dipartimento di Ingegneria Strutturale, Politecnico di Milano, Italy

(*Received* 30 *September* 1996; *in revised form* 25 *June* 1997)

Abstract—The failure of rock-like, quasi-brittle materials is influenced by the development of an intrinsic process zone in the form of a localized region of microcracking. In particular, the process zone has a fundamental importance for defining the structural or system behavior in terms of the post-peak instability, a qualitative size effect, and the maximum stress or material strength, a quantitative size effect. For geometrically similar beams of different sizes, this paper presents experimental evidence from locations of acoustic emissions of the process-zone development, at maximum stress, in terms of shape and size. The experiments suggest that a notch effect developed in the specimens, with assumed uniform tractions being transmitted between the two boundaries of the notch; the radius of curvature of the notch was taken to be one-half the width of the intrinsic process zone. The failure criterion was that at peak load the stress at the notch tip reached the theoretical tensile strength, the so-called characteristic strength of the material. It is shown that the quantitative size effect can be explained by extending the classical Neuber results on stress concentrations around notches through an account of the intrinsic process zone and its cohesive interaction. A notable outcome of the analysis is that two competing factors define the nominal strength of a quasi-brittle material: the positive contribution of the process zone and the competing aspects of the undamaged volume, that is, the size. © 1998 Elsevier Science Ltd. All rights reserved.

1. INTRODUCTION

A fundamental concern in most problems involving stressed materials is the prediction of failure. For ideally brittle or perfectly plastic materials, a stress analysis indicates no dependence on scale: structures of different sizes fail at the same maximum stress. However, it has been shown (for instance, Bažant, 1984) that in materials characterized by microcracking, so-called quasi-brittle materials, the nominal strength—the maximum stress according to elementary methods of strength of materials—evaluated with laboratory specimens of given geometry and load configuration is dependent on size. Due to the existence of a localized zone of microcracking, a structure composed of a quasi-brittle material may fail at a stress quite different, usually smaller but possibly larger, than the strength value determined in the laboratory.

One of the first attempts to explain size effect is credited to Weibull (1939), who investigated the statistics of tensile failure based on fracture extension. He showed that the strength of a material is a function of the volume of the specimen through the application of the weakest link concept. As explained by Bažant and co-workers (Bažant and Xi, 1991; Bažant, 1993), however, the Weibull theory may be inadequate because it ignores the stress redistributions due to localized damage (the process zone) prior to maximum stress. A size effect in fatigue was noticed by Peterson and Wahl (1936), and notch sensitivity was shown to reduce with specimen size. Extensive evidence is available from direct and indirect tensile tests indicating that the apparent or nominal strength is size dependent (for example, Glucklich and Cohen, 1967; Hardy *et al.*, 1973; Swan, 1980; Karihaloo and Nallathambi, 1986; Bažant and Kazemi, 1990; Tang *et al.* 1991). For uniaxial compression, Millard *et*

* Author to whom correspondence should be addressed. Tel.: 001 612 625 9060. Fax: 001 612 626 7750.

al. (1955) and Evans and Pomeray (1958) experimentally observed a strong correlation between size and strength, and suggested a relation in the form

$$\sigma_N = k/a^n, \tag{1}$$

where σ_N is the nominal strength, k and n are constants, and a is the length of a cubic specimen, a characteristic size of the structure. Millard *et al.* (1955) noted that n on the order of 0.5 is expected if existing crack lengths are proportional to the sides of the cubic specimens. The power law relation was later used by Leicester (1969; 1973) to describe the effect of size on the strength of concrete. More recently, dimensionless scaling factors (Cherepanov, 1979; Bažant, 1984) based on fracture mechanics relate the influence of geometrical features to the strength. The size effect law of Bažant (1984, 1993) provides a smooth transition for the size-independent behavior [$n = 0$ in eqn (1)] to the linear fracture mechanics prediction ($n = 0.5$). Other explanations (Chong *et al.*, 1989; Karihaloo and Nallathambi, 1990; Shah and Ouyang, 1994) also have been advanced to explain size effect, all relying on the application of fracture mechanics.

It is evident from experimental observations of quasi-brittle materials that an analysis of the structural behavior and in particular, an evaluation of the nominal strength, require a knowledge of the evolution of microcracking as a function of applied loads. Among the methods used to examine development of microcracks within a test specimen is the acoustic emission technique (for instance, Shah and Labuz, 1995), which is based on the recording of transient elastic waves resulting from the sudden release of energy due to microcracking. Optical methods (Hariharan, 1984) measure only surface deformation of the specimen, while the crack front has been shown to be not rectilinear through a specimen (Swartz and Go, 1984). Acoustic emission seems to be an objective technique to get information on the mechanisms generated in the entire volume.

In this paper, a stress analysis is presented that requires knowledge of the geometric features of the localized zone of microcracking at peak load, referred to as the intrinsic process zone, for justifying the scale effect with respect to strength. Geometrically similar four-point bend beams were considered. The size and shape of the intrinsic process zone were identified through the locations of acoustic emission, and a characteristic length—claimed to be a material parameter—was required for the analysis. It is demonstrated that the strength-size effect can be explained by extending the classical Neuber results on stress concentrations around notches through an account of the process zone and its cohesive interaction. A notable outcome of the analysis is that two competing factors define the nominal strength of a quasi-brittle material: the positive contribution of the microcracked zone and the competing aspects of the undamaged volume, that is, the size.

2. EXPERIMENTAL APPARATUS

Flexural testing of two rocks, Cold Spring (Charcoal) granite and Berea sandstone, was performed to induce tensile failure using prismatic beams of rectangular cross-section in sizes varying by a factor of four. Charcoal granite is a medium grained rock (average grain size of 2 mm), composed mainly of feldspars and quartz; inhomogeneities within this granite are crack-like features, 1 mm in length and smaller (Friedman and Bur, 1974). Young's modulus (E) and Poisson's ratio (ν), greatly influenced by the crack density of about 0.4, are 50 GPa and 0.15 in tension and 55 GPa and 0.18 in compression. The Berea sandstone (99% quartz) tested has a porosity of about 18% and a grain size of 0.2 mm. The existing defects within this rock are pore-like features, and thus the elastic moduli are approximately the same in tension and compression: $E = 16$ GPa and $\nu = 0.28$. The specimen geometry was held constant at a span-to-height (L/H) ratio of 2.67 or 3.0 for large, intermediate, and small sizes; the dimension of the beams in mm (span × height) were about 800×300 and 400×150 for the granite and 900×300 for the sandstone and 200×75 for the granite and sandstone, all with a thickness (T) of 35 mm. The beams were loaded in four-point bending over the middle third of the span, producing a region of

constant moment. Most specimens contained a sawn notch to facilitate post-peak control, although a number of small beams, both granite and sandstone, were tested without a notch to examine its influence on microcracking.

Experiments were conducted in a closed-loop, servo-hydraulic, 1 MN capacity load frame with the feedback signal taken as the displacement measured along the outermost tensile fiber over a 100 mm gage length (for specimens without a notch) or across the sawn notch at a gage length of 15 mm. A strain-gage based transducer monitored the crack mouth opening displacement, which was programmed to increase at a rate of 2×10^{-4} mm/s. One linear variable differential transformer, an LVDT with a linear range of 0.25 mm, was attached to the centerline of the beam to measure the load-point displacement. Test control and data acquisition were provided by a microcomputer.

3. ACOUSTIC EMISSION

Acoustic emission (AE) can be detected at the surface of a specimen by a transducer that converts an acoustic-pressure pulse into an electrical signal of very small amplitude. The major element of an AE transducer is a piezoelectric ceramic mounted with little backing, so that the response is under damped. At the optimum sensitivity, the voltage generated by a 1-μbar acoustic pressure has a typical value of 0.3 mV. For laboratory studies on materials such as rock and concrete, transducers that are sensitive between 0.1 and 2 MHz are recommended, because the frequencies of most emissions are included in this band width.

An acoustic emission system has been designed around CAMAC (Computer Automated Measurement And Control) based, high speed, data acquisition equipment manufactured by LeCroy Corporation (Chestnut Ridge, New York). The instrumentation consisted of four, two-channel modular transient recorders (LeCroy model 6840) with a sampling rate of 20 million points per second (50 nanoseconds between points) and 8-bit resolution. The system was designed to capture 64 events with 2 kbytes per event (about 100 μs) as fast as they arrived. An important aspect to identify the intrinsic process zone through locations of AE is to record a large number of events without interruption. The total transfer time for 64 events, including the storage time on a microcomputer for post-processing, was about 4 s, yielding an effective sampling rate of 16 events/s.

The AE system accommodated eight piezoelectric transducers (Physical Acoustics model S9225). These sensors, with a radius of 3 mm, were mounted directly to the material with a methyl-cyanoacrylate glue and catalyst; a consistent coupling procedure reduced the variability in bonded-transducer response. The entire wave forms were stored automatically and sequentially on a hard disk. Preamplifiers (40 dB gain) and filters (band pass 0.1 to 1.2 MHz) were chosen to maximize amplification, minimize noise, and assure matched frequency response. Typically, the noise at the output of the preamplifiers was around 2 mv. In order to capture events with high signal-to-noise ratios so that spurious events would not be included, the trigger level was set at 7 mv. A pretrigger of 50 μs allowed the entire wave form to be recorded. (It is necessary to examine the signal before the trigger point to identify the first arrival.) By knowing these relative arrival times, the P-wave velocity of the material, and the coordinates of each sensor, the event hypocenter can be estimated (Salamon and Weibols, 1974; Labuz *et al.*, 1996). Only locations with an error of 2.5 mm or less were considered.

4. EXPERIMENTAL RESULTS

The conditions at peak stress, with regard to the development of the intrinsic process zone, were established from tests on specimens with a smooth boundary, that is, no notch. For the granite beam, locations of acoustic emission up to about 95% of the maximum stress indicated no localized activity (Fig. 1a); the microseismic events were distributed randomly within the region of constant moment. The picture was different, however, when the AE hypocenters were determined around peak stress (Fig. 1b). Localization was clearly identified within a zone approximately 15 mm long $\times$ 10 mm wide. The results were similar

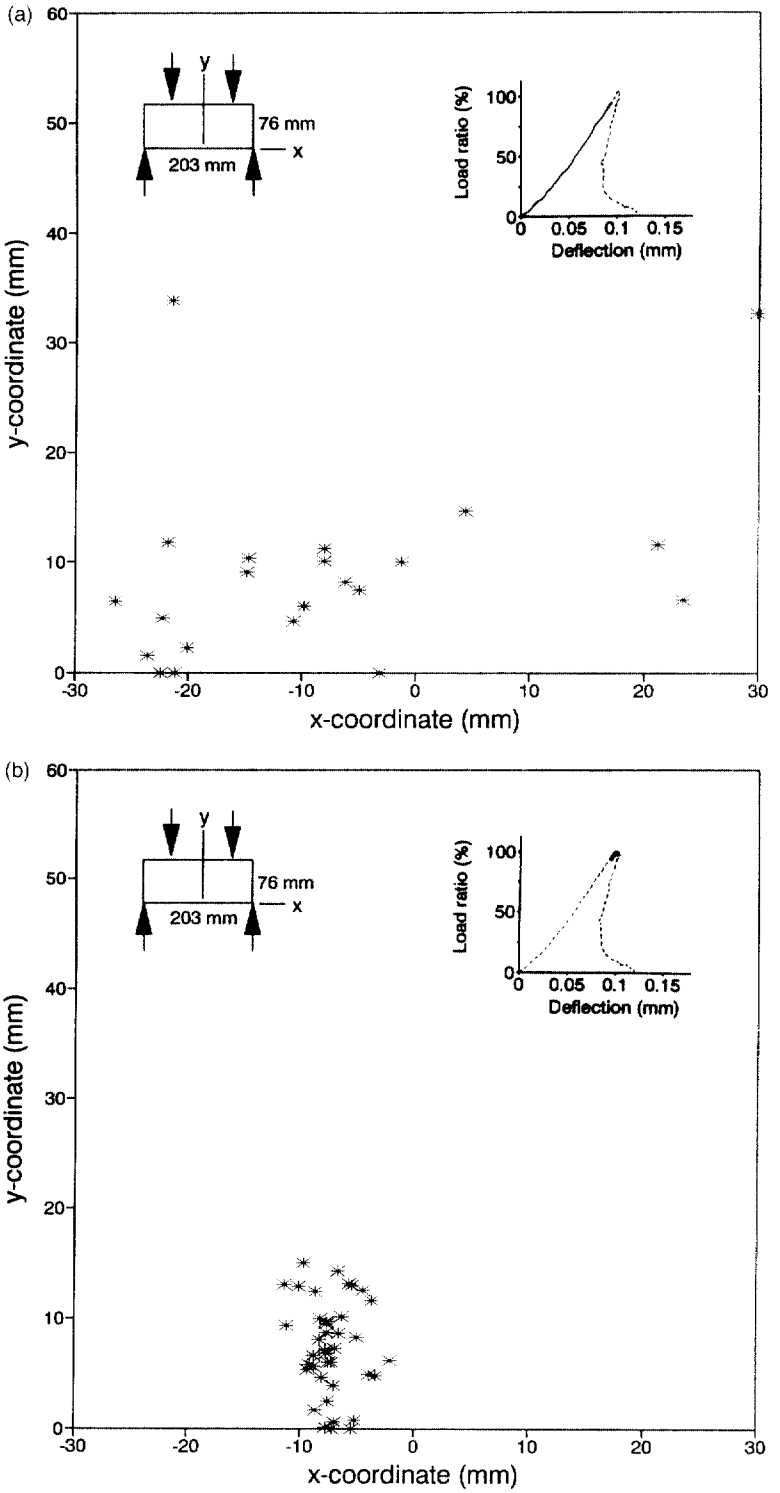

Fig. 1. Locations of acoustic emission in small beams (75 mm height) with a smooth boundary (no notch). a. Granite beam before peak load. b. Intrinsic process zone in granite beam. c. Intrinsic process zone in sandstone beam.

for the smooth sandstone beam (Fig. 1c) in that an intrinsic process zone formed at peak load, although the zone for the smaller-grained rock was about 5 mm wide. For both specimens, it was observed after the test that the AE locations corresponded very well to the path of the visible fracture.

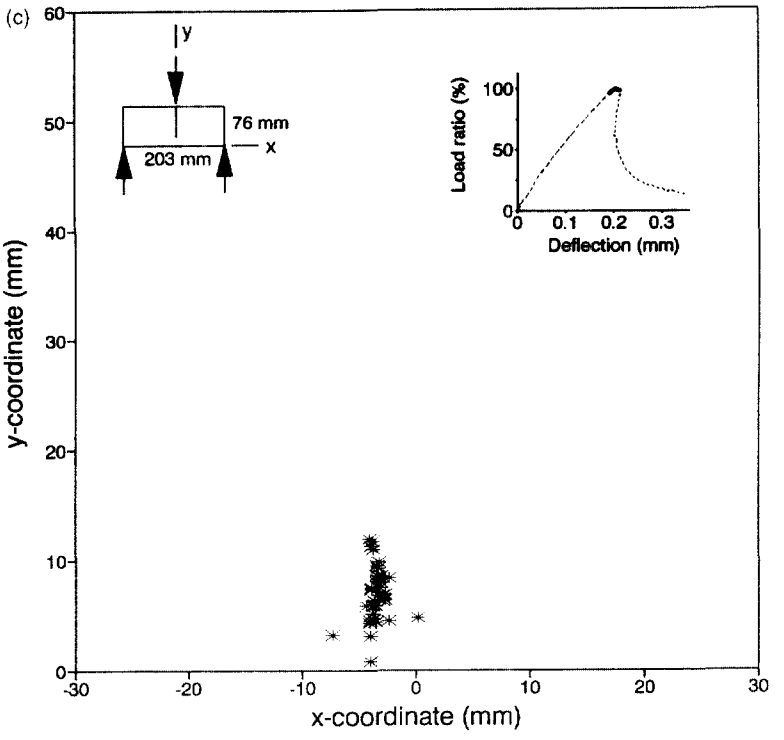

Fig. 1. —*Continued.*

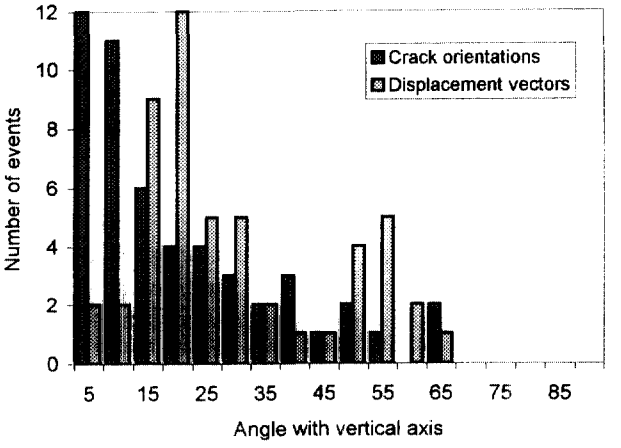

Fig. 2. Orientation of microcracks associated with the intrinsic process zone of the small sandstone beam (Fig. 1c).

The orientation of microcracking was examined through an estimation of the source mechanism (Shah and Labuz, 1995). With the assumption of a point source of displacement discontinuity and with proper system calibration, it is possible to determine two directions, one associated with the orientation of the microcrack and the other associated with the displacement vector. Thus, the normal to the crack plane cannot be determined uniquely, although it can be inferred from the loading. The source characterization of AE from the smooth sandstone beam (Fig. 1c) indicated two sets of possible microcrack orientations, one predominantly vertical and the other subvertical (Fig. 2). By considering the stress field in the beam, it can be expected that the majority of the microcracks would be vertical. Therefore, Fig. 2 (as drawn) may be representative of the microcrack development, which confirmed that the microcracking was preferential.

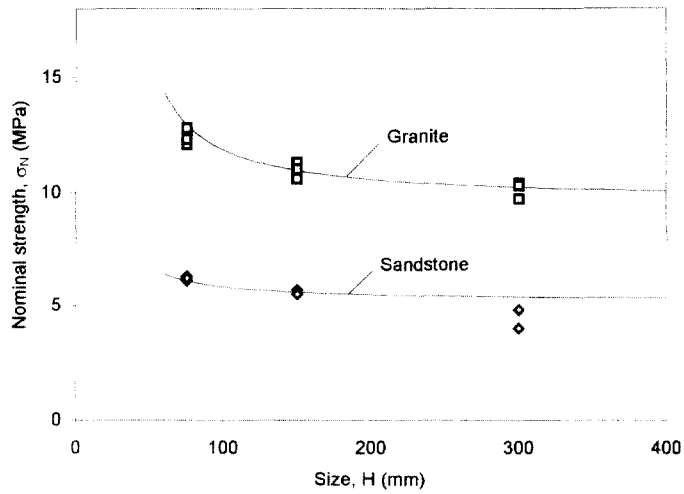

Fig. 3. Size effect displayed by notched beams.

For beams, the nominal strength σ_N of the material, that is, the maximum allowable stress evaluated according to the elementary methods of classical beam theory, can be defined by

$$\sigma_N = M/S, \tag{2}$$

where M is the maximum bending moment and S is the elastic section modulus. From the small beams with no notch, the nominal strengths for the granite and the sandstone were 12.8 and 6.3 MPa. From experiments on small beams with notches, the maximum stresses were 12.3 MPa for the granite and 6.2 MPa for the sandstone. Thus, the presence of a notch did not appear to significantly influence the strength of these quasi-brittle materials (Labuz *et al.*, 1985). To simplify testing, 2.5-mm long notches were sawn in the small beams, while notches 5 and 10 mm in length were cut in the intermediate and large beams. The quantitative size effect for the notched beams is displayed in Fig. 3; the nominal strength is a decreasing function of the size.

The development of the process zone from the notched beams may be considered at different stages of loading. For instance, at approximately 85% of the peak stress, the large sandstone beam showed (Fig. 4a) a clustering of AE events mainly near the notch within a width of 5 mm. With additional load application, the concentration of AE activity moved further away from the notch, indicating damage evolution (Fig. 4b); the width of the zone, however, was approximately the same, about 5 mm. Near peak load, the intrinsic process zone was developed (Fig. 4b). Similar results, with regard to AE development, were obtained for the intermediate and small sandstone beams at different stages of loading. The AE locations around peak load for a large (notched) granite beam (Fig. 4c) indicated an intrinsic process zone about 10 mm wide, again very similar to the results from the intermediate and small granite beams.

In summary, the AE activity around peak stress for the notched beams of different sizes indicated similar process zone lengths, possibly influenced by the stress gradient of the different sizes beams, but the widths were approximately the same. Thus, for the sizes considered, it appeared that the dimensions of the intrinsic process zone, particularly the width, may be a material characteristic related to grain size and porosity/microcrack density of the material. Furthermore, it is claimed that the intrinsic process zone is important for identifying the theoretical strength of quasi-brittle materials, and should be considered for the determination of a nominal strength.

5. STRESS ANALYSIS

To interpret the characteristic strength of a quasi-brittle material, and the related problem of the change in nominal strength with size, an approach is suggested that considers

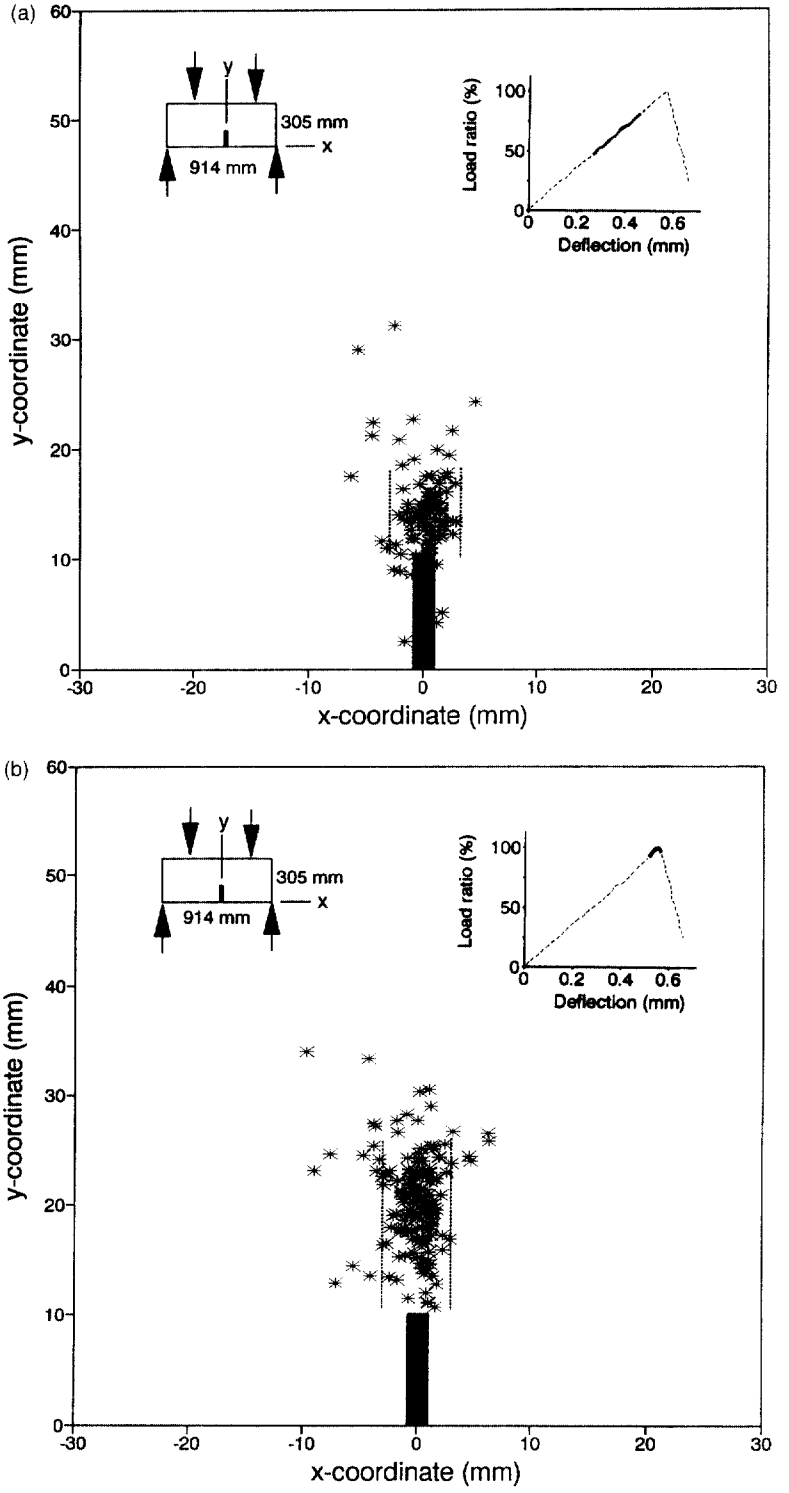

Fig. 4. Locations of acoustic emission in large beams (300 mm height) with a notch; the process-zone width is indicated by the dotted lines. a. Sandstone beam, up to 85% of peak load. b. Intrinsic process zone in sandstone beam. c. Intrinsic process zone in granite beam.

a separation of the original and damaged volumes of the material. In this way, the undamaged portion forms a notched structure—the notch is a consequence of the intrinsic process zone—with tractions due to some type of cohesive interaction, and this notched structure controls the peak stress. For the granite, the intrinsic process zone was 15–20 mm in length

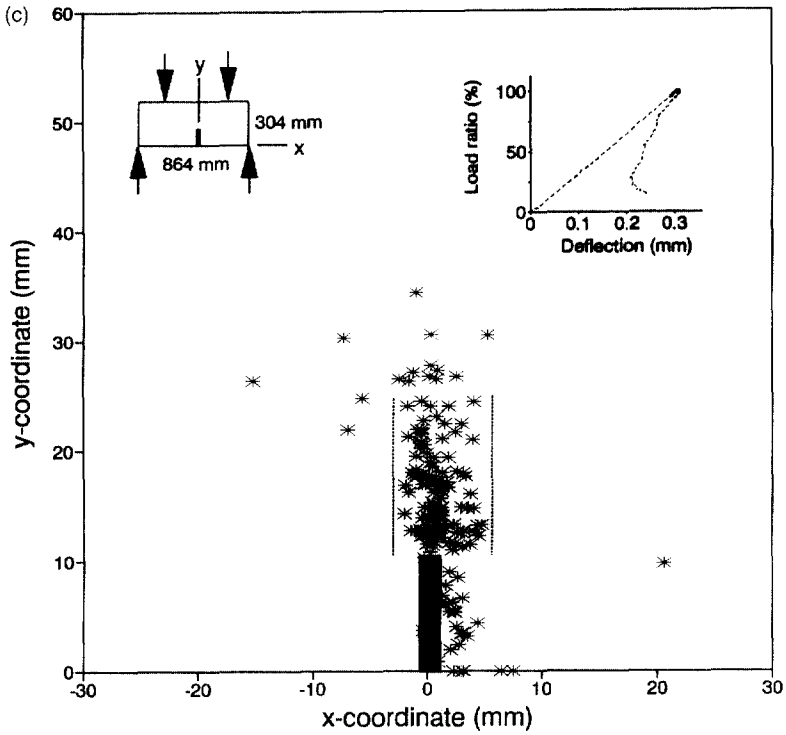

Fig. 4.—*Continued.*

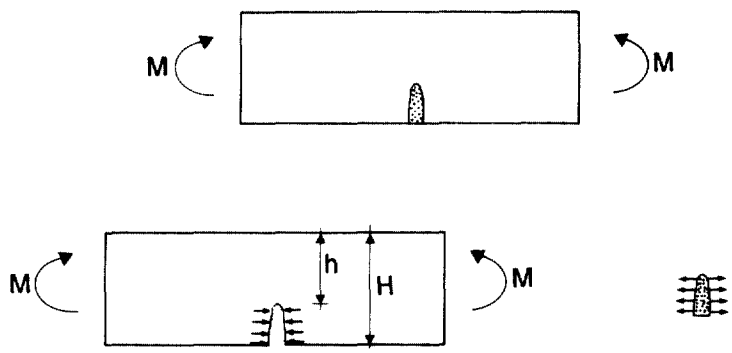

Fig. 5. Model of the conditions at peak load: a beam with a cohesive notch.

and 8–12 mm in width (Figs 1b and 4c). For the sandstone, the intrinsic process zone was 12–17 mm long and 5 mm side (Figs 1c and 4b). The length may be influenced by the stress state in the specimen, but the width displayed a characteristic features that will be interpreted as a characteristic length of the material (Bažant and Pijaudier-Cabot, 1989).

In general, the acoustic emission locations showed that a small volume becomes further microcracked upon reaching peak stress. For a typical specimen, the volume of the intrinsic process zone was orders of magnitude smaller than the volume of the structure. To capture the essential behavior, some simplification of the problem may be justified with respect to the geometry of the process zone and its cohesive interaction. Thus, the experiments suggest that a notch effect is developed in a specimen, with tractions being transmitted between the two boundaries of the notch (Fig. 5); the radius of curvature of the notch is taken to be one-half the width of the process zone. The failure criterion adopted was that of maximum principal stress: at peak load the stress at the notch tip reaches the theoretical tensile strength σ_t, the so-called characteristic strength of the material. Solutions for notched bodies under the fundamental states of stress (axial force, bending moment, pure shear,

and torsion) were presented by Neuber (1937) within the framework of linear elasticity. In addition, the material must be homogeneous, a good approximation because the dimensions of the specimen were large compared to the grain size of the material.

5.1. *Notch effect*

To find a solution that holds at peak stress and that satisfies equilibrium, a decomposition of the problem was considered. If uniform traction within the process zone can be assumed, then the solution is obtained with a superposition of the following three problems (Fig. 6):

(1) a notched beam with a bending moment, M, without cohesive interaction along the notch (the fundamental stress field);
(2) a uniform tensile traction, equal to the theoretical tensile strength of the material, imposed on the boundary of the notched beam and equilibrated with a tensile force, N;
(3) a notched beam with a compressive force $-N$ that balances the tensile force.

In this way, the original problem is statically equivalent to the addition of the three considered problems. Note that conditions (2) and (3) represent the perturbation of the fundamental stress field due to the intrinsic process zone.

As already stated, the tensile stress at the notch tip is assumed to be equal to the theoretical tensile strength of the material σ_t at peak load:

$$\sigma_t = \sigma_{(1)} + \sigma_{(2)} + \sigma_{(3)}, \tag{3}$$

where $\sigma_{(1)}$, $\sigma_{(2)}$, and $\sigma_{(3)}$ are the horizontal normal stresses at the notch tip for the three conditions.

For the considered decomposition,

$$\sigma_{(2)} = \sigma_t \tag{4}$$

$$N = \sigma_t HT, \tag{5}$$

where T and H are the thickness and the height of the beam. Therefore, eqn (3) reduces to

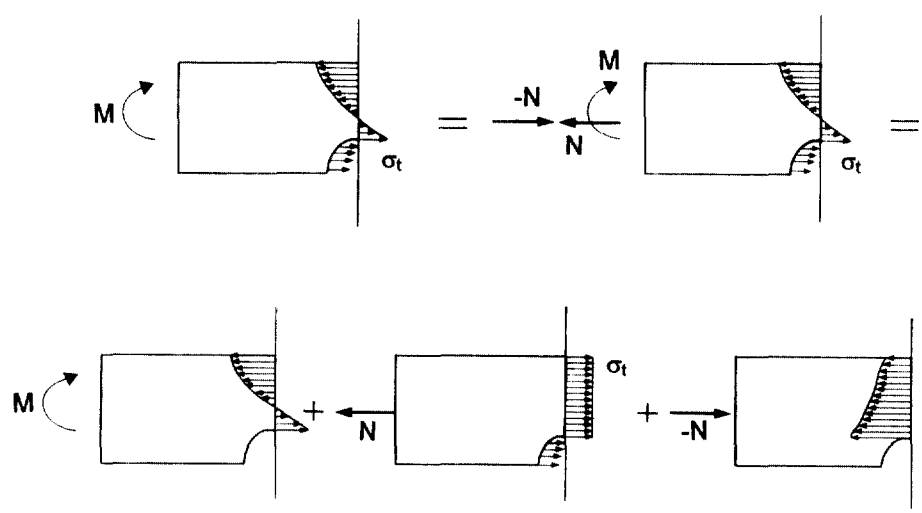

Fig. 6. Decomposition of the model.

$$\sigma_{(1)} + \sigma_{(3)} = 0. \tag{6}$$

It may be shown (Neuber, 1937), assuming a shallow notch of hyperbolic shape, that the stress at the tip of the notch $\sigma_{(1)}$ produced by the bending moment M may be written

$$\sigma_{(1)} = (M/S) f_1(h/\rho), \tag{7}$$

where $f_1(h/\rho)$ is a function of the ratio between the ligament height h and the radius of curvature of the notch tip ρ, taken as one-half the process-zone width. Moreover, the stress $\sigma_{(3)}$, produced by the compressive force $-N$ is

$$\sigma_{(3)} = -(N/hT) f_2(h/\rho), \tag{8}$$

where $f_2(h/\rho)$ is a different function of h/ρ.

Considering eqn (5), it follows that

$$\sigma_{(3)} = -\sigma_1 (H/h) f_2(h/\rho). \tag{9}$$

From eqns (7) and (9), eqn (6) can be written

$$\sigma_N = \sigma_1 (H/h) F(h/\rho), \tag{10}$$

where σ_N is the nominal strength defined by eqn (2) and $F(h/\rho)$ is the ratio f_2/f_1. If $\beta = h/\rho$, then the function $F(\beta)$ is given by

$$F(\beta) = \frac{3\{(\beta)^{1/2}[1 - 3\beta(1+\beta)^{1/2} + 2\beta] - (1 - \beta - \beta^2)(\arctan \beta^{1/2})\}}{\beta\{\beta^{1/2}[1 - (1+\beta)^{1/2}] + (1 + \beta \arctan \beta^{1/2}\}}. \tag{11}$$

Figure 7, a plot of eqn (11), reveals that with ratios of h/ρ greater than ten, the function reaches an asymptotic value approximately equal to 0.74. A logarithmic plot with

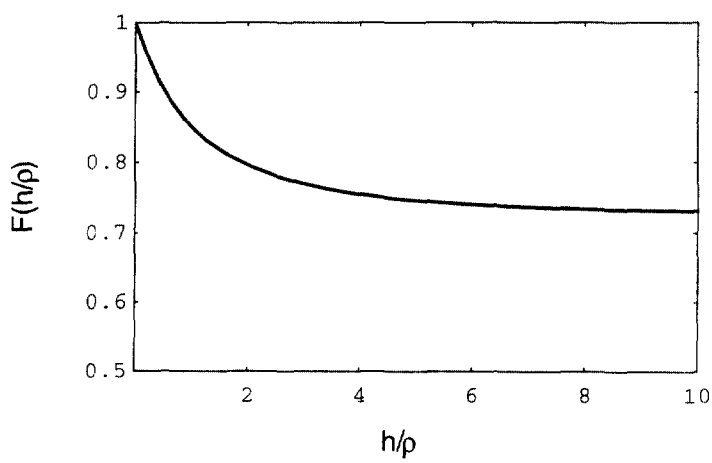

Fig. 7. Reduction factor for a beam with a notch of radius ρ.

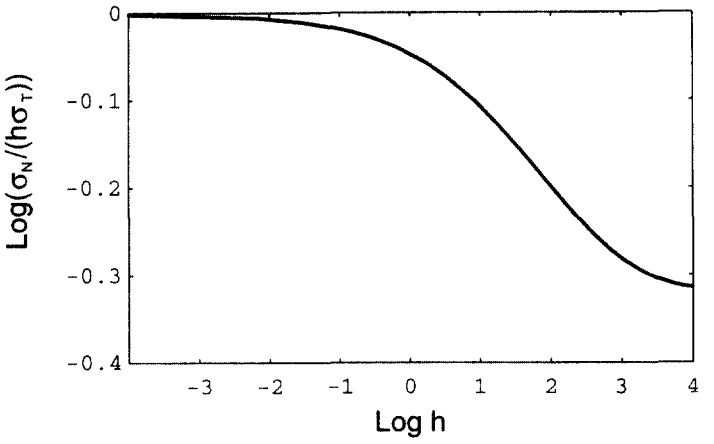

Fig. 8. Size effect predicted for a beam with an intrinsic process zone length of 15 mm and a width of 10 mm (radius of 5 mm).

$H-h = 15$ mm (Fig. 8) illustrates the general size effect law (similar to, for instance, Bažant, 1993) for a quasi-brittle material, with the additional feature of constant nominal strength for very large structures, assuming a constant value of the process-zone width ($\rho = 5$ mm).

5.2. *Discussion*

From the size effect eqn (10), note that the nominal strength depends not only on the theoretical tensile strength of the material, but also on the cohesive interaction (as measured by the ratio between the beam height H and the undamaged ligament h) and the notch effect induced by the intrinsic process zone (as measured by the function F that depends on the undamaged ligament and the radius of the notch tip). Indeed, the two factors compete in defining the nominal strength of a specimen composed of a quasi-brittle material; the ratio H/h is the amplification factor due to the cohesive interaction of the process zone, whereas the function F is the reduction coefficient that represents the perturbation in the stress field due to the shape and size of the undamaged volume. The ratio H/h, which is always greater than one, is the measure of the positive contribution of the process zone to the nominal strength. From the experiments reported on granite, the ratio is 1.05 for the large beam and 1.26 for the small beam with $\rho = 5$ mm and $H-h = 15$ mm. The analysis suggests that the variation of the nominal strength in these tests was primarily due to the influence of the process zone.

The size effect displayed by a quasi-brittle material may be related to the width of the process zone, which is viewed as an intrinsic material length: brittle materials are characterized by a small value of the width. For quasi-brittle materials, it is possible to consider specimens that are large, such that value of ligament height h allow the function F to approach the lower limit of the nominal strength, which for specimens under pure bending is about 75% of the theoretical strength. Furthermore, as the material becomes less brittle (the intrinsic length increases), the specimen size that is needed to determine the lower limit of the nominal strength for a given test geometry must increase. It may be observed that when the ligament length is sufficiently small compared to the process zone (assuming that the analysis for a shallow notch is still valid), the nominal strength evaluated according to eqn (2) may be larger than the theoretical tensile strength of the material. In this case, it is possible to assert that the inelasticity of the process zone becomes dominant with respect to the notch effect that is created by the localization.

Finally, the size effect eqn (10) is based on a mechanical approach manifested through the features of the intrinsic process zone: $\rho = 5$ mm, $H-h = 15$ mm for granite and $\rho = 2.5$ mm, $H-h = 12$ mm for sandstone. If the tests on the small beams with a smooth boundary are used to evaluate the nominal strength σ_N, and the geometric features of the process zone are known (as measured by the AE technique), it is possible to determine the true

tensile strength of the material: σ_t was about 13 MPa for the granite and about 7 MPa for the sandstone. The size effect eqn (10) can then by compared with the experimental results in Fig. 3, and reasonable agreement between theory and data is shown.

6. CONCLUSIONS

Acoustic emission (AE) seemed to be a viable technique to identify the localization at peak load, the so-called intrinsic process zone. From bend tests on laboratory specimens, the AE locations showed that a small volume became further microcracked upon reaching peak stress. For a typical beam, the volume of the process zone was orders of magnitude smaller than the volume of the specimen. It appeared that the development of the process zone could be idealized as a notch within the structure, with uniform cohesive tractions being transmitted between the two boundaries of the notch. The radius of curvature of the notch was taken to be one-half the width of the process zone, which may be related to a characteristic length of the material.

The proposed stress analysis showed that the nominal strength of a quasi-brittle material depended not only on the theoretical tensile strength, but also on the size of the process zone (with respect to the beam size) and the radius of the notch tip. The two factors compete in defining the nominal strength: the cohesive interaction of the process zone can amplify the theoretical strength while the perturbation in the stress field from the notch effect can reduce the strength. The size effect displaced by a quasi-brittle material can be related to width of the process zone: brittle materials will be characterized by a small value of the width. Furthermore, large specimens can be considered such that the nominal strength approaches a lower limit, which for specimens under pure bending is about 75% of the theoretical strength. Thus, as the material becomes less brittle (the intrinsic length increases), the specimen size that is needed to determined the lower limit of the nominal strength for a given test geometry must increase.

Acknowledgement—Partial support was provided by the National Science Foundation Grant No. CMS-9532061 and the North Atlantic Treaty Organization Collaborative Research Grant No. 950695.

REFERENCES

Bažant, Z. P. (1984) Size effect in blunt fracture: concrete, rock, metal. *Journal of Engineering Mechanics, ASCE* **110,** 518–535.

Bažant, Z. P. (1986) Mechanics of distributed cracking. *Applied Mechanics Review* **39,** 675–705.

Bažant, Z. P. (1993) Scaling laws in mechanics of failure. *Journal of Engineering Mechanics, ASCE* **119,** 1828–1844.

Bažant, Z. P. and Kazemi, M. T. (1990) Determination of fracture energy, process zone length and brittleness number from size effect, with application to rock and concrete. *International Journal of Fracture* **44,** 111–131.

Bažant, Z. P. and Pijaudier-Cabot, G. (1989) Measurement of characteristic length of nonlocal continuum. *Journal of Engineering Mechanics, ASCE* **115,** 755–767.

Bažant, Z. P. and Xi, Y. (1991) Statistical size effect in quasibrittle structures. *Journal of Engineering Mechanics, ASCE* **117,** 2623–2640.

Cherepanov, G. P. (1979) *Mechanics of Brittle Fracture*, p. 570. McGraw-Hill, New York.

Chong, K. P., Li, V. C. and Einstein, H. H. (1989) Size effects, process zone and tension softening behavior in fracture of geomaterials. *Engineering Fracture Mechanics* **34,** 669–678.

Evans, I. and Pomeroy, C. D. (1958) The strength of cubes of coal in uniaxial compression. *Mechanical Properties of Non-metallic and Brittle Material*, ed. W. H. Walton pp. 5–28. Butterworths, London.

Friedman, M. and Bur, T. R. (1974) Investigation of the relations among residual strain, fabric, fracture and ultrasonic velocity in rocks. *Int. J. Rock Mech. Min. Sci.* **11,** 221–234.

Glucklich, J. and Cohen, L. J. (1967) Size as a factor in the brittle-ductile transition and the strength of some materials. *International Journal of Fracture Mechanics* **3,** 278–289.

Hardy, M. P., Hudson, J. A. and Fairhurst, C. (1973) The failure of rock beams, Part I—Theoretical studies. *Int. J. Rock Mech. Min. Sci.* **10,** 53–67.

Hariharan, P. (1984) Optical Holography: Principles, Techniques and Applications. Cambridge University Press.

Karihaloo, B. L. and Nallathambi, P. (1986) Determination of specimen-size independent fracture toughness of plain concrete. *Magazine of Concrete Research* **38,** 67–76.

Karihaloo, B. L. and Nallathambi, P. (1991) Notched beam test: mode I fracture toughness. *Fracture Test Methods for Concrete*, ed. S. P. Shah and A. Carpinteri, pp. 1–86. Chapman and Hall, London.

Labuz, J. F., Shah, S. P. and Dowding, C. H. (1985) Experimental analysis of crack propagation in granite. *Int. J. Rock Mech. Min. Sci. Geomech Abstr.* **22,** 85–98.

Labuz, J. F., Dai, S.-T. and Shah, K. (1996) Identifying failure through locations of acoustic emission. *Transportation Research Record* **1526,** 104–111.

Leicester, R. H. (1969) The size effect of notches. *Proceedings of the 2nd Australian Conference Mechanics of Structures and Materials*. pp. 4.1–4.20. Melbourne.

Leicester, R. H. (1973) Effect of size on the strength of structures. *Division of Building Research Paper* 71, CSIRO, pp. 1–13. Melbourne.

Millard, D. J., Newmann, P. C. and Phillips, J. W. (1955) The apparent strength of extensively cracked materials. *Proc. Phys. Soc. London* B68, 723–728.

Neuber, H. (1937) *Kerbspannungslehre*. Springer-Verlag OHG, Berlin.

Peterson, R. E. and Wahl, A. M. (1936) Two- and three-dimensional cases of stress concentration, comparison with fatigue tests. *Journal of Applied Mechanics Transactions of ASME*, A15–A22.

Salamon, M. D. G. and Wiebols, G. A. (1974) Digital location of seismic events by an underground network of seismometers using the arrival times of compressional waves. *Rock Mech.* **6,** 141–166.

Shah, K. R. and Labuz, J. F. (1995) Damage mechanisms in stressed rock from acoustic emission. *J. Geophys. Res.* **100**(B8), 15,521–15,539.

Shah, S. P. and Ouyang, C. (1994) Fracture mechanics for failure of concrete. *Annu. Rev. Mater. Sci.* **24,** 293–320.

Swan, G. (1980) Fracture stress scale effects for rocks in bending. *Int. J. Rock Mech. Min. Sci. & Geomech. Abstr.* **17,** 317–324.

Swartz, S. E. and Go, C. G. (1984) Validity of compliance calibration to cracked concrete beams in bending. *Exp. Mech.* **24,** 129–134.

Tang, T., Shah, S. P. and Ouyang, C. (1991) Fracture mechanics and size-effect of concrete in tension. *J. Struct. Engng, ASCE* **118,** 3169–3185.

Weibull, W. (1939) A statistical theory of the strength of materials. *Ingvetensk.*